Kinetics of ballistic annihilation and branching

Pierre-Antoine Rey
Theoretical Physics, Oxford University, 1 Keble Road, Oxford OX1 3NP, United Kingdom

Michel Droz
Département de Physique Théorique, Université de Genève, CH-1211 Genève 4, Switzerland

Jarosław Piasecki
Institute of Theoretical Physics, Warsaw University, Hoża 69, Pl-00 681 Warsaw, Poland
(Received 21 August 1998)

We consider a one-dimensional model consisting of an assembly of two-velocity particles moving freely between collisions. When two particles meet, they instantaneously annihilate each other and disappear from the system. Moreover, each moving particle can spontaneously generate an offspring having the same velocity as its mother with probability $1-q$. This model is solved analytically in the mean-field approximation and studied by numerical simulations. It is found that for $q=1/2$ the system exhibits a dynamical phase transition. For $q<1/2$, the slow dynamics of the system is governed by the coarsening of clusters of particles having the same velocities, while for $q>1/2$ the system relaxes rapidly towards its stationary state characterized by a distribution of small cluster sizes. [S1063-651X(99)00501-2]

PACS number(s): 82.20.Mj, 05.20.Dd

I. INTRODUCTION

Ballistically controlled reactions provide simple examples of nonequilibrium systems with complex kinetics and have recently attracted a lot of interest [1–9]. They consist of an assembly of particles moving freely between collisions with given velocities. When two particles meet, they instantaneously annihilate each other and disappear from the system.

Depending on the initial velocity distribution, two classes of asymptotic states have been observed in one-dimensional systems. In general, for continuous initial velocity distribution [3,10], as well as for some special case of discrete velocity distribution (symmetric two-velocity distribution [1,2,5] or symmetric trimodal velocity distribution with a sufficiently small fraction of immobile particles [6,7]), the steady state turns out to be empty and it is approached algebraically in time. The dynamical exponent characterizing the time decay depends on the initial velocity distribution and it is still not completely clear how to characterize the universality classes for this problem [10]. On the contrary, for some discrete velocity distribution, the stationary state may not be empty, but may contain particles moving all with the same velocity (for example nonsymmetric bimodal velocity distribution [1,5] or a trimodal velocity distribution with more than 25% of particles initially at rest [6,7]). This noninteracting state is generally approached with an exponentially fast decay.

A richer behavior can be expected in a system with, in opposition to the ballistic annihilation case, an interacting steady state. This can be achieved by constantly bringing new particles in the system by some suitable mechanism. A possibility is to allow branching processes: ballistically moving particles can spontaneously generate, with a given branching rate, some offsprings. Accordingly, one speaks of ballistic branching annihilation.

The problem of branching annihilation has been recently studied in the framework of a diffusive dynamics [11,12]. The simplest example of such a system would be one with a single species of particle A, undergoing diffusive behavior, single-particle annihilation $A\to\varnothing$, and branching $A\to 2A$. There is always a trivial absorbing state, with no particles. For sufficiently low branching rate, this is the only stationary state, but for larger values of this rate, another nontrivial ''active'' stationary state appears. This stationary-state phase transition belongs to the directed percolation universality class [13]. A slightly more complicated class of model are reaction-diffusion systems with the underlying reaction processes $2A\to\varnothing$ and $A\to(m+1)A$, with m even. It turns out that for these models the critical exponents are not the ones of directed percolation but belong to a new universality class [11,12] characterized by branching and annihilating walks with an even number of offsprings. The constraint of local ''parity'' conservation is the reason for the existence of this new universality class.

Our aim here is to study the problem of ballistic branching annihilation (BBA) in one dimension for which interesting new properties can be foreseen. The paper is organized as follows. In Sec. II, the BBA model is defined. The exact dynamical equations of motion are derived for the one-dimensional case. In Sec. III, the dynamics of the model is studied within a mean-field-like approximation. In particular, the phase diagram of the steady state is established in terms of the different parameters of our model. In this approximation, the steady state is always approached exponentially fast. Section IV is devoted to numerical simulations of the one-dimensional model. It is shown that fluctuations play a crucial role. Indeed, as in the mean-field approximation, a phase transition occurs when the probability that the offspring takes the velocity of its mother is $q=1/2$; however, for $q<1/2$ the dynamics is governed by the coarsening of clusters of particles having the same velocity, and the system approaches a completely filled stationary state with a power-

law decay. For $q>1/2$, there is no coarsening and the system relaxes rapidly towards a nonfilled stationary state. Finally, the results are discussed in Sec. V.

II. THE MODEL

We shall first define precisely the BBA model studied and second derive the corresponding equations of motion.

A. Definition of the model

We consider a one-dimensional system composed of particles of size σ initially uniformly randomly distributed in space. Moreover, at $t=0$, the velocities of the particles are random independent variables distributed with the symmetric bimodal distribution:

$$P(v)=\frac{1}{2}[\delta(v-c)+\delta(v+c)]. \tag{1}$$

The dynamics consists of two mechanisms: (a) The ballistic annihilation: Two particles making contact (with opposite velocities) disappear instantaneously. (b) The branching: during the time interval $[t,t+dt]$, the following branching processes take place: (i) A particle with coordinates (position and velocity) (x,c) produces with probability $p(1-q)dt$ a pair of particles with coordinates $(x-\sigma,c)$ and (x,c); (ii) A particle with coordinates (x,c) produces with probability $pqdt$ a pair of particles with coordinates $(x-\sigma,-c)$ and (x,c); (iii) A particle with coordinates $(x,-c)$ produces with probability $p(1-q)dt$ a pair of particles with coordinates $(x,-c)$ and $(x+\sigma,-c)$; (iv) A particle with coordinates $(x,-c)$ produces with probability $pqdt$ a pair of particles with coordinates $(x,-c)$ and $(x+\sigma,c)$. (The particular choice of the position of the newly created particle has been made in order that, independent of its velocity, a child cannot collide with its mother at birth.) Thus the parameter $0\leqslant p\leqslant\infty$ characterizes the overall branching rate, while the parameter $0\leqslant q\leqslant 1$ characterizes the probability that the offspring has a velocity opposed to that of its mother. The particular case $p=0$ corresponds to the pure ballistic annihilation problem previously studied [1,2,5,6].

B. Exact equations of motion

We can now derive the equations of motion describing the dynamics of the system. In the particular case $p=0$, a kinetic equation for the two-particle conditional distribution of nearest neighbors was derived as a rigorous consequence of the dynamics of ballistic annihilation [5,6]. This equation completely described the evolution of the system when initially higher-order conditional distributions factorized into products of two-particle ones. It was then possible to extract exactly and analytically the long time behavior of the particle density for several velocity distributions. Unfortunately, this property is no longer valid in the case with branching. Having not been able to find an observable in which one is able to reproduce this exact closure, one has to face the usual problem of dealing with a complete hierarchy of coupled equations [14]. It seems thus hopeless to find an exact analytical solution to these equations. Accordingly we shall only write the equation for the one-particle density distribution $\rho_1(x,v;t)$. In Sec. III, this equation will be solved using a mean-field approximation.

A careful bookkeeping of the possible dynamical processes leads to the following equations:

$$(\partial_t+c\partial_x)\rho_1(x,c;t)=-2c\rho_2(x,c;x+\sigma,-c;t)+pq\left(\rho_1(x-\sigma,-c;t)-\sum_{v=\pm c}\int_0^\sigma dy\,\rho_2(x-\sigma,-c;x+y,v,t)\right)$$
$$+p(1-q)\left(\rho_1(x+\sigma,c;t)-\sum_{v=\pm c}\int_0^\sigma dy\,\rho_2(x-y,v;x+\sigma,c;t)\right), \tag{2}$$

and

$$(\partial_t-c\partial_x)\rho_1(x,-c;t)=-2c\rho_2(x,c;x+\sigma,-c;t)+pq\left(\rho_1(x+\sigma,-c;t)-\sum_{v=\pm c}\int_0^\sigma dy\,\rho_2(x-y,v;x+\sigma,c;t)\right)$$
$$+p(1-q)\left(\rho_1(x-\sigma,-c;t)-\sum_{v=\pm c}\int_0^\sigma dy\,\rho_2(x-\sigma,-c;x+y,v;t)\right), \tag{3}$$

where $\rho_2(x_1,v_1;x_2,v_2;t)$ is the joint two-particle density to find a particle in the state (x_1,v_1) simultaneously with another in the state (x_2,v_2) at time t.

The right-hand side of Eq. (2) can be interpreted in the following way: the first term describes the annihilation of a particle (x,c) with a particle of opposite velocity. It is given by the product of the density of a collision configuration $[\sigma\rho_2(x,c;x+\sigma,-c,t)]$ with the frequency of such an encounter $(2c/\sigma)$. The second term describes the branching of a particle of velocity $-c$, at position $x-\sigma$, giving birth to a particle of velocity $+c$ at position x. This is only possible if no other particles are present in the interval $[x,x+\sigma]$ (otherwise there will be an overlap between two particles) and it happens with the rate pq. Finally, the third term describes the creation with rate $p(1-q)$ of a particle whose mother has the same velocity. The same restriction as in the previous case applies.

One can in principle write the equation of motion for ρ_2

along the same lines. However, we shall not give here this cumbersome equation, as we are not going to use it.

For simplicity, we shall only consider a spatially homogeneous system. We can thus write $\rho_1(x,v;t)=\rho_1(v,t)$ and $\rho_2(x_1,v_1;x_2,v_2;t)=\rho_2(x_1-x_2,v_1;0,v_2;t)$. Introducing then the observable $\Psi(t)\equiv\rho_1(c,t)-\rho_1(-c,t)$, one easily shows that it is an exactly conserved quantity when $q=1/2$. This feature reflects the particular choice of rule, which is precisely symmetric when $q=1/2$. As a consequence, one expects our model to exhibit a particular behavior at this point.

III. MEAN-FIELD ANALYSIS

A first attempt to obtain information about our model is to apply a mean-field approximation on Eqs. (2) and (3). One then assumes the following factorization:

$$\rho_2(x_1,v_1;x_2,v_2;t)=\rho_1(x_1,v_1;t)\rho_1(x_2,v_2;t)=\rho_1(v_1,t)\rho_1(v_2,t) \tag{4}$$

(the last equality holds for a spatially homogeneous system).

It is then suitable to introduce in addition to the variable Ψ the second variable,

$$\Phi(t)\equiv\rho_1(c,t)+\rho_1(-c,t). \tag{5}$$

Equations (2) and (3) lead to

$$\frac{d\Phi}{dt}=p(1-\sigma\Phi)\Phi-c(\Phi^2-\Psi^2) \tag{6}$$

and

$$\frac{d\Psi}{dt}=p(1-2q)(1-\sigma\Phi)\Psi. \tag{7}$$

The formal solution of this last equation is

$$\Psi(t)=\Psi(0)\exp\left[p(1-2q)\left(t-\sigma\int_0^t d\tau\,\Phi(\tau)\right)\right], \tag{8}$$

As before, one sees that the value $q=1/2$ plays a special role. Indeed, two regimes have to be distinguished.

(i) For $0\leqslant q<1/2$: the exponential term diverges unless $(1-\sigma\Phi)\to 0$ as $t\to\infty$. Thus a possible stationary solution is

$$\Phi_s=\frac{1}{\sigma},\quad \Psi_s^2=\frac{1}{\sigma^2}. \tag{9}$$

In the particular case $q=0$, the time-dependent solution can be obtained explicitly as shown in the Appendix. For $t\to\infty$, one recovers the above stationary solution.

(ii) For $1/2<q\leqslant 1$: in this case, a possible stationary solution is

$$\Psi_s=0,\quad \Phi_s=\frac{1}{\sigma}(1+c/p\sigma)^{-1}. \tag{10}$$

It is straightforward to verify that the above stationary solutions are stable and are approached exponentially in time.

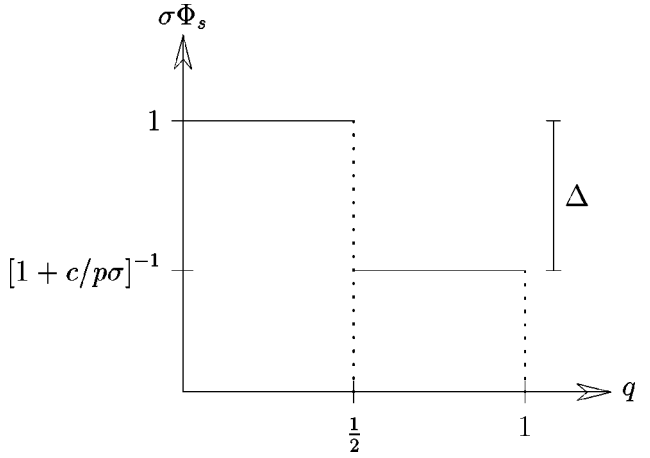

FIG. 1. Mean-field phase diagram: the stationary value of the averaged density Φ_s is plotted against q for a fixed value of p.

Moreover, when $q=1/2$ the complete time dependent solution can be obtained. From Eq. (7), one indeed finds $\Psi(t)=\text{const}=\Psi_0$, and thus Eq. (6) becomes

$$\frac{d\Phi}{dt}=p\Phi-(c+p\sigma)\Phi^2+c\Psi_0^2, \tag{11}$$

whose solution reads

$$\Phi(t)=\frac{p}{2(c+p\sigma)}+\frac{\gamma A\cosh(At)+A(c+p\sigma)\sinh(At)}{A\cosh(At)+\gamma(c+p\sigma)\sinh(At)}, \tag{12}$$

with $A=p^2/4+c(c+p\sigma)\Psi_0^2$ and $\gamma=\Phi(0)-p/[2(c+p\sigma)]$. The stationary state is then given by $\Psi_s=\Psi_0$ and

$$\Phi_s(q=1/2)=[p+\sqrt{p^2+4c(c+p\sigma)\Psi_0^2}]/(c+p\sigma). \tag{13}$$

Here again, one sees from Eq. (12) that the steady state is approached in an exponential way. As already noted, $\Psi(t)$ is an exactly conserved quantity for $q=1/2$.

The mean-field stationary phase diagram is shown in Fig. 1. The stationary value Φ_s is plotted against q for a fixed value of $p\neq 0$. The interesting feature is the presence of a gap $\Delta(p)$ for $q=1/2$ given by

$$\Delta(p)=\frac{1}{\sigma}\left(1-\frac{1}{1+c/p\sigma}\right). \tag{14}$$

$\Delta(p)$ decreases as p increases. When $q<1/2$, $\Phi_s=1/\sigma$ for all values of p (completely filled state), while for $q>1/2$, Φ_s increases monotonically with p. The dependence is linear for small p, but $\Phi_s\to 1/\sigma$ when $p\to\infty$.

IV. NUMERICAL SIMULATIONS

In view of the situation when $p=0$ [1,2,5], one can anticipate that the fluctuations will also play an important role in the case with branching. One way to deal with the complete problem, including fluctuations, is to perform numerical simulations.

The simulations were performed for a one-dimensional periodic lattice with typically 2^{17} sites. The velocity of each

particle was drawn from a symmetric bimodal distribution. However, on computational grounds, the particle velocities were chosen to be $(0,c')$ (with $c'>0$). The results for our model defined in Sec. II can be recovered by performing a simple Galilean transformation and setting $c=c'/2$. The particle size σ is the lattice spacing and the discretized time step is given by $\tau=\sigma/c'$.

The algorithm used to simulate the dynamics is the following. During one time step τ, the following three processes occur sequentially.

(1) Ballistic motion: independent of the occupation state of the sites, the particles with velocity c' move one site to the right.

(2) Annihilation: two particles located on the same site disappear.

(3) Branching: for each remaining particle, one draws two random numbers, r_p and r_q, uniformly distributed in the interval $[0,1]$. One offspring particle is added to the left (right) nearest neighbor of a particle with velocity c' (0) if the site is empty and if r_p is less than a given value $\tilde{p}$. Hence, $\tilde{p}$ is the probability of branching. This new particle takes the velocity of its mother with a certain probability $1-q$, i.e., if $r_q>q$ (and the other velocity otherwise). If two particles are created on the same site (thus born from two different mothers), they annihilate instantaneously.

For each of the above steps, the sites were updated simultaneously. The simulations were run on a Connection Machine CM-200 and the data averaged over 10 independent realizations. The mean initial density for all the simulations was 0.5, with, on average, the same densities of both kinds of particles. We have also shown that our results obtained for a lattice of 2^{17} sites were free of finite-size effects.

Note that when a particle branches, it can create at most one particle during a time step τ. As a consequence, this limits the value of p that can be explored through the simulations. Indeed, the branching rate p is related to $\tilde{p}$ via

$$\tilde{p}=p\tau. \tag{15}$$

Thus using the definition of τ and c', one finds

$$\frac{p\sigma}{c}=2\tilde{p}. \tag{16}$$

$\tilde{p}$ being a probability, the adimensional branching rate $p\sigma/c$ can only take values between 0 and 2.

We can now discuss the numerical data obtained using the above algorithm. Two kinds of quantities have been investigated: first, the time-dependent density with particular emphasis on the stationary states and the way these stationary states are approached; second, a more microscopic quantity, namely the time-dependent cluster-size distribution $P(l,t)$ in the system and some of its moments. These quantities are well suited to describe the coarsening process present in the system.

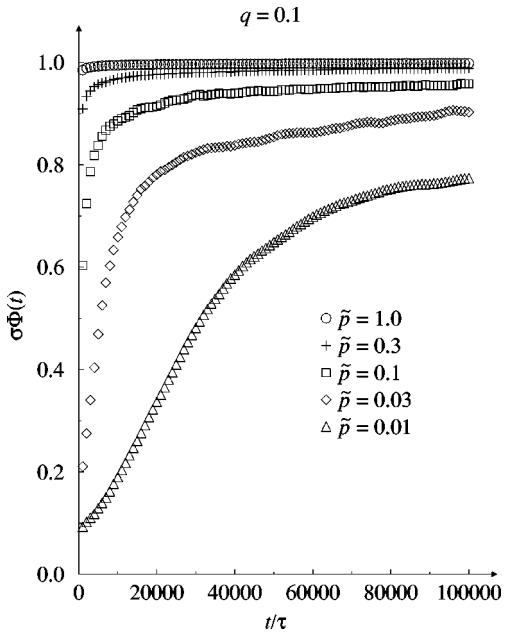

FIG. 2. Time evolution of the particle density $\sigma\Phi(t)$ as a function of time t for $q=0.1$ and several values of $\tilde{p}$.

As in the mean-field approach and as expected from the last remark of Sec. II, the value $q=1/2$ turns out to play a particular role and three regimes have to be distinguished.

(i) For $0\leqslant q<1/2$: The time evolution of the particle density $\Phi(t)$ is shown in Fig. 2 for several values of $\tilde{p}$. Clearly, the system reaches a stationary state $\Phi_s=1/\sigma$ in agreement with the mean-field prediction. However, as shown in Fig. 3, the stationary state is approached as $\Phi_s-\Phi(t)\sim t^{-1/2}$. This power law is established after a crossover time roughly proportional to $1/p$.

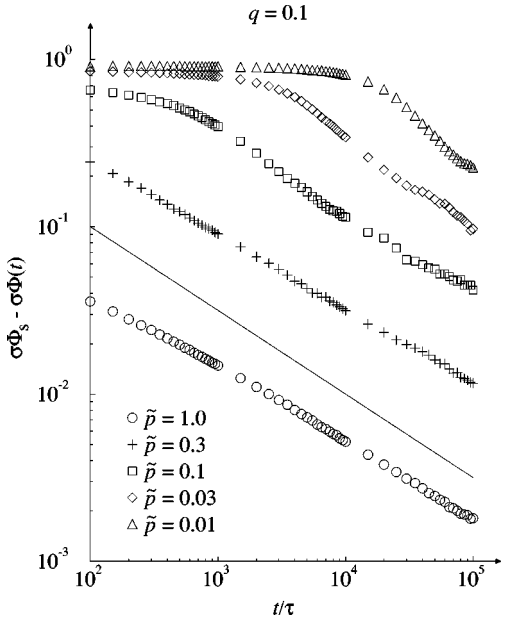

FIG. 3. $\sigma\Phi_s-\sigma\Phi(t)$ versus t in a double logarithmic scale, for $q=0.1$ and several values of $\tilde{p}$. For comparison, the full line represents $t^{-1/2}$. This decay is established after a crossover time which behaves as $\tau/\tilde{p}$.

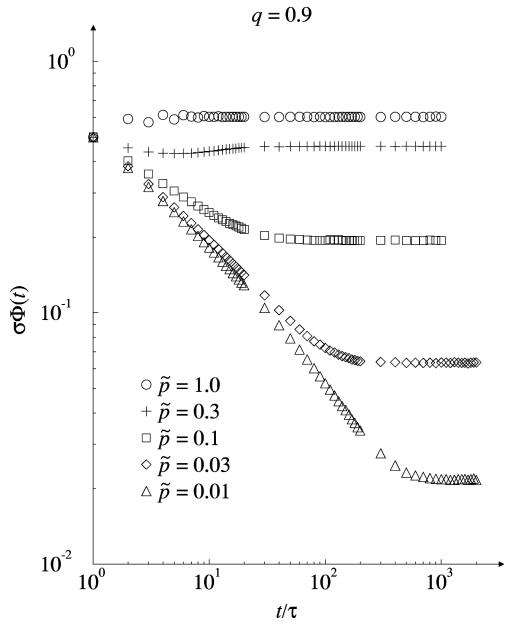

FIG. 4. Time evolution of the particle density $\sigma\Phi(t)$ as a function of time t for $q=0.9$ and several values of $\tilde{p}$. The stationary state is reached after a time of order $10\tau/\tilde{p}$.

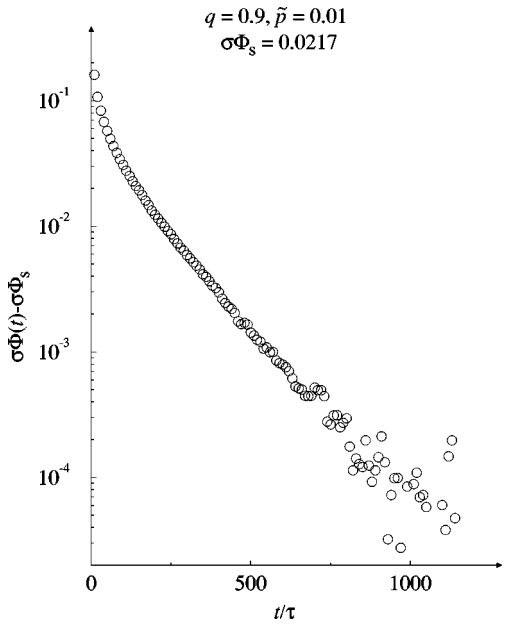

FIG. 6. Semilogarithmic plot of $\sigma\Phi(t)-\sigma\Phi_s$ versus t for $q=0.9$ and $\tilde{p}=0.01$. The exponential approach towards the steady state is established for $t/\tau\simeq 250$.

(ii) For $1/2<q\leqslant 1$: The time evolution of the particle density $\Phi(t)$ is shown in Fig. 4 for several values of $\tilde{p}$. As depicted in Fig. 5, the stationary value of the density depends both on $\tilde{p}$ and q. For $\tilde{p}<0.1$, it is well fitted by

$$\Phi_s(\tilde{p},q)\approx\tilde{p}\exp(0.55/q). \tag{17}$$

Moreover, for $\tilde{p}$ large enough Φ_s is not increasing monotonically as a function of $\tilde{p}$, but Φ_s exhibits a maximum and then slightly decreases as $\tilde{p}$ increases. As shown in Fig. 6, the stationary state is approached in an exponential way according to $\Phi_s-\Phi(t)\sim\exp(-A\tilde{p}t)$, where A may depend on q.

(iii) The limit case $q=1/2$ is more difficult to investigate due to the slow decay towards the stationary state. In fact for $\tilde{p}>0.3$, there is evidence that the stationary state is completely filled, i.e., $\Phi_s=1/\sigma$. For smaller values of $\tilde{p}$ the simulations do not allow us to draw any conclusions, as shown in Fig. 7. Nevertheless, for $q<1/2$, one has Φ_s

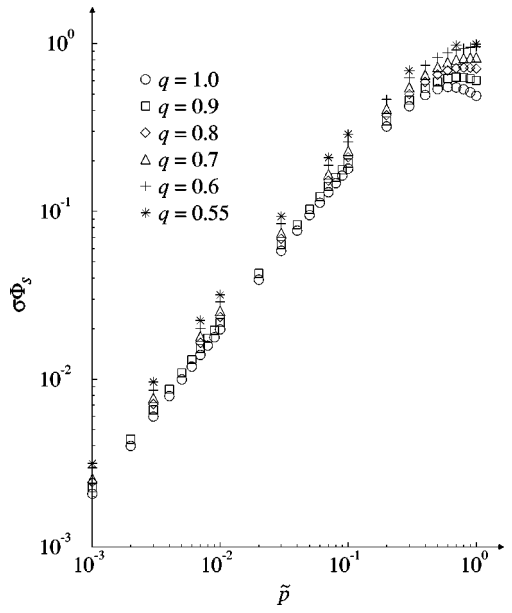

FIG. 5. The stationary values of the averaged density $\sigma\Phi_s$ are plotted against $\tilde{p}$, for several values of $q>1/2$, obtained by numerical simulations.

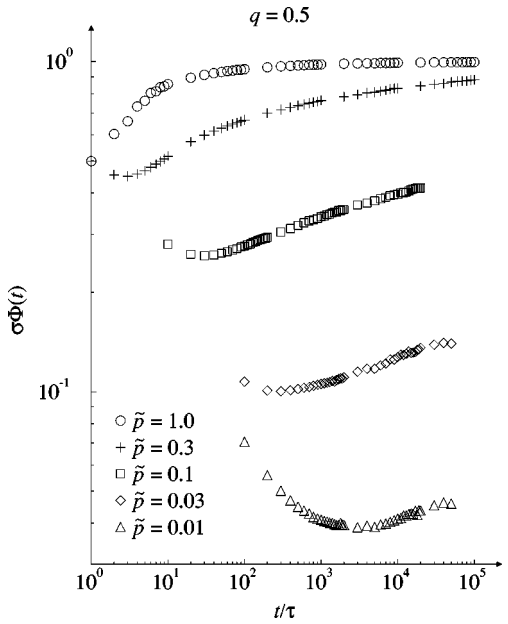

FIG. 7. Time evolution of the particle density $\sigma\Phi(t)$ as a function of time t for $q=0.5$ and several values of $\tilde{p}$. For small values of $\tilde{p}$ (less than 0.3), we are unable to extract the steady-state density, for CPU reasons.

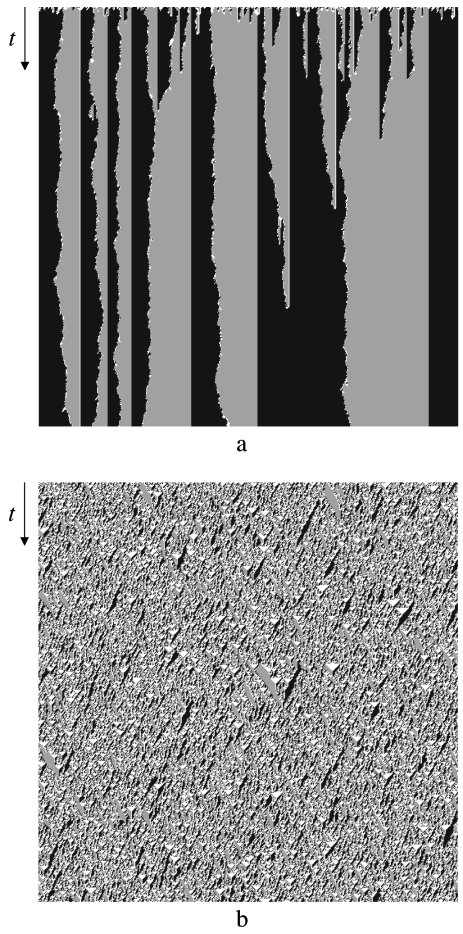

FIG. 8. Time evolution (vertical axes) of the configurations for a chain of 512 sites (the initial density is approximately one-half) and for 1024 time iterations. The white pixels indicate sites without particle, the gray ones sites with a particle towards the right, and the black ones sites with a particle moving towards the left. (a) is for $\tilde{p}=0.7$ and $q=0.9$, while (b) is for $\tilde{p}=0.7$ and $q=0.1$.

$=1/\sigma$ for all values of $\tilde{p}$ while for $q>1/2$, Eq. (17) shows that, at least for small $\tilde{p}$, $\Phi_s \neq 1/\sigma$. Thus for small $\tilde{p}$, Φ_s has a jump at $q=1/2$, and we believe that such a jump will be present for all finite values of p.

We can now consider the properties of the clusters present in the system at a given time. The qualitative situation is well illustrated by the two snapshots in Fig. 8. They represent the time evolution of a 512-site system during 1024 iterations. Moreover, a change of reference frame has been performed such that the particle velocities appear to be $\pm c$. Depending on q, one observes totally different pictures. In the case $\tilde{p}=0.7, q=0.1$ [Fig. 8(a)], large clusters (of similar particles) are present. They are separated by two types of interfaces: vertical ones (which are stable) and rough ones. The dynamics of the system is totally governed by the random walks of the rough interfaces. During the time evolution, one rough interface may collide with a stable interface leading to the coalescence of two clusters into a large one. In the case $\tilde{p}=0.7, q=0.9$ [Fig. 8(b)], the sizes of the clusters are rather small and there are no stable interfaces. The dynamics is of a different type.

A more quantitative description is given by the investigation of the time-dependent cluster-size distribution $P(l,t)$. In the domain $0 \leqslant q < 1/2$, where coarsening is observed, one expects [15] that $P(l,t)$ will obey a scaling form:

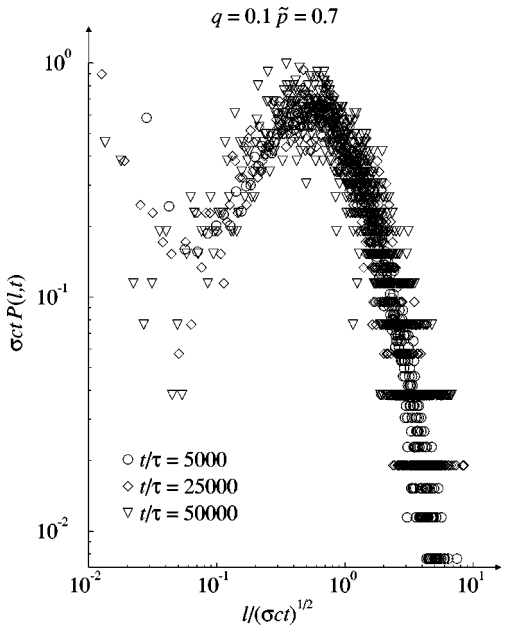

FIG. 9. Scaling form of the cluster-size distribution for $\tilde{p}=0.7, q=0.1$. $P(l,t)t^{\alpha}$ is plotted versus $lt^{-\beta}$ for $\alpha=1$ and $\beta=0.5$.

$$P(l,t) \sim t^{-\alpha} \Pi(lt^{-\beta}). \tag{18}$$

In Fig. 9, we plot the scaling function obtained by the collapse of the data for $\tilde{p}=0.7, q=0.1$, with $\alpha=1$ and $\beta=0.5$. Although the plot is very noisy, one still notes that the scaling function $\Pi(z)$ has a very particular shape, with a sharp maximum at $z=z_{max}$. The value of z_{max} increases slowly with q, going from 0.4 for $q=0.1$ to 1.2 for $q=0.4$.

A better way to extract the exponents α and β is to consider the nth-order moments of the distribution defined as

$$\langle l^n \rangle = \frac{\int_{\sigma}^{\infty} dl\, l^n P(l,t)}{\int_{\sigma}^{\infty} dl\, P(l,t)}, \tag{19}$$

which according to the scaling form given by Eq. (18) should behave as

$$\langle l^n \rangle \sim t^{\alpha_n} = t^{n\beta}, \tag{20}$$

while

$$\int_{\sigma}^{\infty} dl\, P(l,t) \sim t^{-\alpha+\beta}. \tag{21}$$

Thus, the above two relations allow us to determine the exponents α and β. The values of α_n for $n=1, \ldots, 6$ are shown on Fig. 10 for $p=0.7$, $q=0.1$. A good fit is obtained for $\beta=0.48\pm0.02$ and $\alpha=0.96\pm0.04$, in very good agreement with our collapsed plot. By repeating our analysis for

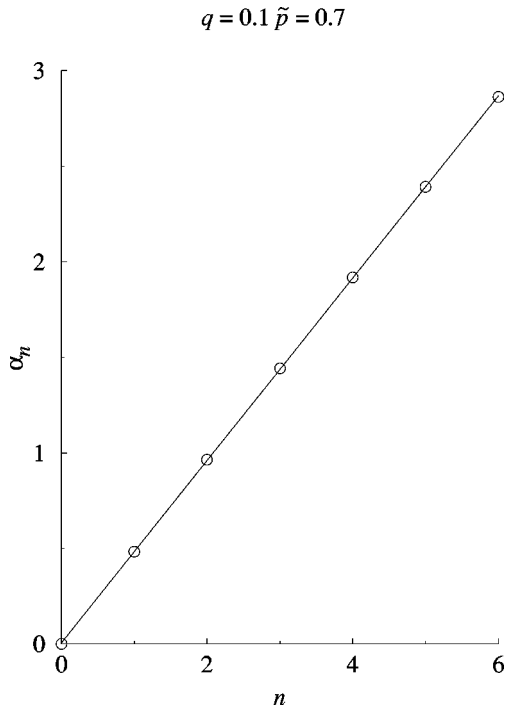

FIG. 10. Exponent α_n (open circles) of the nth moment of the cluster distribution function for $n=0,\ldots,6$ and $\tilde{p}=0.7, q=0.1$. The line is the fit $\alpha_n = 0.01 + 0.48n$.

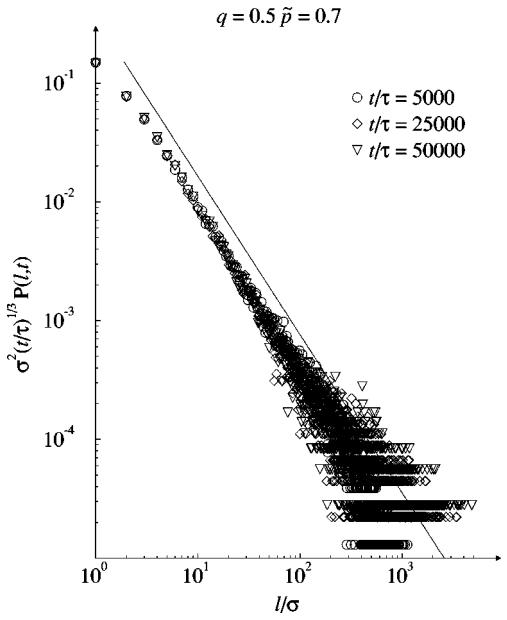

FIG. 11. Scaling form of the cluster-size distribution for $\tilde{p}=0.7, q=0.5$. $P(l,t)t^{1/3}$ is plotted versus l in a double logarithmic scale. The full line represents $l^{-4/3}$.

other values of q (namely, 0.2, 0.3, and 0.4), the same values for the exponents fit reasonably well the data.

For $q=1/2$, the different moments of the cluster-size distribution are $\alpha_1=0.33$, $\alpha_2=0.96$, $\alpha_3=1.60$, $\alpha_4=2.22$, $\alpha_5=2.82$, and $\alpha_6=3.40$. These exponents are of the form $\alpha_n = -0.26 + 0.61n$ which is not compatible with the relation (20). This probably shows that the simulations have not yet reached the true asymptotic regime. Moreover, as shown in Fig. 11, $P(l,t)$ is of the form

$$P(l,t) \sim t^{-1/3} l^{-4/3}, \tag{22}$$

over two decades in the variable l. Note that Eq. (22) cannot be valid for arbitrarily large l, because the moments of $P(l,t)$ diverge with the upper limit of integration.

Finally, in the domain $1/2 < q \leqslant 1$, where no coarsening is observed, the system approaches very rapidly its stationary state and no dynamical scaling has been found for the cluster distribution. However, in the stationary state, the cluster distribution takes the form

$$P(l) = C_1 \exp(-C_2 l), \tag{23}$$

where C_1 and C_2 are two constants.

V. INTERPRETATION OF THE RESULTS AND CONCLUSIONS

The first interesting point is the particular role played by the value $q=1/2$. As already mentioned in Sec. II, for $q=1/2$, one notes the presence of an extra conservation law in the system. The difference between the average local density of particles with positive and negative velocities is strictly zero. It is well known that conservation law has a great influence on the dynamics of nonequilibrium statistical systems. Accordingly, one may expect that the dynamics in $q=1/2$ is particular.

In view of the scaling properties of the problem, it may be useful to think about it in terms of a dynamical renormalization group. Based on the results of both the mean-field approximation and the numerical simulations, one is led to conjecture the presence of three fixed points in this system: an unstable ''critical'' fixed point at $q=1/2$ and two attractive fixed points at $q=0$ and $q=1$.

When $q<1/2$, the branching processes favors the apparition of a pair of consecutive particles with the same velocities and the dynamics is governed by the attractive fixed point at $q=0$. Large particle clusters with opposite velocities are formed during the time evolution and two kinds of interfaces are present in the system [see Fig. 8(a)]. First, let us consider the interface between two clusters of colliding particles and call this type of interface I_1. Such an interface has a very long life. Indeed, the probability that a vacancy present at one of the extremities of a cluster of size L traverses the cluster and perturbates the interface is of the order of $(1-p)^L$. Thus, an interface I_1 is very stable in the long time limit where the system is made up of large clusters. The second type of interface, called I_2, separates noncolliding clusters. Thus it does not necessarily have a one-site extension, but it can be wider. Hence, its behavior is more subtle. Three different regimes may be considered. The simplest case to discuss is when $p\sigma/c>1$. In this case, the interface I_2 is typically formed by only one empty lattice site, whose dynamics is diffusive. Indeed, one can show that both boundaries of an interface I_2 perform a Brownian motion. Moreover, when $p\sigma/c>1$, this random walk is biased, so that both boundaries tend to come closer together. For sufficiently long time, the initial gap separating two noncolliding clusters will shrink to one single site, which will perform a random walk. Eventually, this hole will encounter an

I_1 interface, permitting the coalescence of two clusters into a larger one. The random walk aspect of this dynamics is responsible for the slow approach towards the stationary state (in $t^{-1/2}$) observed in the simulations. When $p\sigma/c=1$, the boundaries of an interface I_2 both perform an unbiased random walk. Accordingly, the initial gap between two noncolliding clusters will not, on average, vary. However, because of the BBA dynamics, this gap will eventually shrink to a single site, either through the creation of a cluster inside the gap when $q\neq 0$, or through the coalescence of two interfaces. Thus the previous argument holds. Finally, when $p\sigma/c<1$, the situation is similar: although the boundaries of I_2 perform a biased random walk which tends to increase the separation between the two noncolliding clusters, the coalescence of two interfaces or a creation of a new cluster inside the gap (if $q\neq 0$) will fill up this space in a more efficient way.

Eventually, the stationary state is completely filled, only one cluster remains and the annihilation process is no longer in effect. For values of q not too far from 1/2, this asymptotic behavior will shows up only for very long times. Accordingly, the results of the (finite time) numerical simulations may still be affected by the properties of the critical fixed point at $q=1/2$, and the dynamics will exhibit some crossover behavior.

In the situation $q>1/2$, a majority of pairs of particles with opposite velocities are created during branching. Due to the annihilation processes, those particles will prevent the formation of large clusters of particles. One may anticipate that the long time dynamics is governed by the other attractive fixed point corresponding to $q=1$. The dynamics is no longer governed by the coarsening mechanism but only by the dynamics of small clusters, hence fast (exponential-like) relaxation occurs. Depending upon the value of p, there is a more or less important fraction of empty sites (or holes) into the system. The presence of these two different dynamical regimes explains the jump observed in the stationary density at $q=1/2$.

This paper shows once again that the mean-field results generally do not hold for low-dimensional systems. Whereas the mean-field approximation predicts the exact critical value for q (because the mean-field equation for Ψ is exact when $q=1/2$) and the right stationary value of the density when $q<1/2$, it is unable to give satisfactory results for the density stationary value for $q>1/2$ (see Figs. 1 and 5). Unsurprisingly, the mean-field approximation is also unable to predict the power-law approach to the stationary state when $q<1/2$, which is obviously governed by fluctuations. More surprisingly, its prediction of an exponentially fast approach towards the steady state when $q>1/2$ is (qualitatively) well verified. However, to better understand this problem, it would be useful to be able to find an exact analytical solution at least for the three fixed-point cases ($q=0$, $1/2$, and 1 for arbitrary values of p) as a support to the above qualitative picture. Unfortunately, we were not able until now to find such exact solutions.

In conclusion, one sees that this simple BBA problem with one offspring exhibits already a very rich behavior. The case with two or more offsprings is a completely open question.

ACKNOWLEDGMENTS

The work was partially supported by the Swiss National Science Foundation (M.D). Two of us (P.-A.R. and J.P.) acknowledge the hospitality of the Department of Theoretical Physics of the University of Geneva where part of this work was done. P.-A.R. was supported by the Swiss National Science Foundation and J.P. acknowledges financial support by the KBN (Committee for Scientific Research, Poland) under Grant No. 2 P03 B 035 12.

APPENDIX

In this Appendix, we give an explicit solution to the mean-field equations (5) and (6) for the case $q=0$. Equations (5) and (6) lead to

$$\Psi\frac{d\Phi}{dt}-\Phi\frac{d\Psi}{dt}=-c\Psi(\Phi^2-\Psi^2). \tag{A1}$$

By multiplying Eq. (A1) by Ψ^{-2}, one finds

$$\frac{d}{dt}\left(\frac{\Phi}{\Psi}\right)=-c\Psi\left[\left(\frac{\Phi}{\Psi}\right)^2-1\right]. \tag{A2}$$

Let us introduce $\chi(t)=\Phi(t)/\Psi(t)$. Equation (A2) becomes

$$\frac{1}{\chi^2-1}\frac{d}{dt}\chi=-c\Psi, \tag{A3}$$

whose solution is

$$\chi(t)=\frac{1+\chi(0)+[\chi(0)-1]\exp\left(-c\int_0^t\Psi(\tau)d\tau\right)}{1+\chi(0)-[\chi(0)-1]\exp\left(-c\int_0^t\Psi(\tau)d\tau\right)}. \tag{A4}$$

If $\chi(0)=\pm 1$, then $\chi(t)=\pm 1$ and one finds $\Psi(t)=\pm\Phi(t)$ for all times, where $\Psi(t)$ obeys

$$\frac{d\Psi}{dt}=p(1\mp\sigma\Psi)\Psi, \tag{A5}$$

whose solution is

$$\Psi(t)^{-1}=\pm\sigma+\exp(-pt)[\Psi(0)^{-1}\mp\sigma]. \tag{A6}$$

Note that in these particular cases, only particles with velocity $+c$ (or $-c$) are present in the system at all times.

If $\chi(0)\neq 1$, one finds

$$\frac{d\Psi}{dt}=p(1-\sigma\Phi)\Psi=p\left\{1-\left[\frac{1+\chi(0)+[\chi(0)-1]\exp\left(-c\int_0^t\Psi(\tau)d\tau\right)}{1+\chi(0)-[\chi(0)-1]\exp\left(-c\int_0^t\Psi(\tau)d\tau\right)}\right]\sigma\Psi\right\}\Psi. \tag{A7}$$

As $|\Psi(t)|$ is a nondecreasing function of time, when $t\to\infty$, the square brackets in Eq. (A7) approach ± 1 depending on the sign of $\chi(0)$. Thus, Eq. (A7) reduces to Eq. (A5).

[1] Y. Elskens and H. L. Frisch, Phys. Rev. A **31**, 3812 (1985).
[2] J. Krug and H. Spohn, Phys. Rev. A **38**, 4271 (1988).
[3] E. Ben-Naim, S. Redner, and F. Leyvraz, Phys. Rev. Lett. **70**, 1890 (1993).
[4] P. L. Krapivsky, S. Redner, and F. Leyvraz, Phys. Rev. E **51**, 3977 (1995).
[5] J. Piasecki, Phys. Rev. E **51**, 5535 (1995).
[6] M. Droz, P.-A. Rey, L. Frachebourg, and J. Piasecki, Phys. Rev. Lett. **75**, 160 (1995).
[7] M. Droz, P.-A. Rey, L. Frachebourg, and J. Piasecki, Phys. Rev. E **51**, 5541 (1995).
[8] J. Piasecki, P.-A. Rey, and M. Droz, Physica A **229**, 515 (1996).
[9] P.-A. Rey, M. Droz, and J. Piasecki, Eur. J. Phys. **18**, 213 (1997).
[10] P.-A. Rey, M. Droz, and J. Piasecki, Phys. Rev. E **57**, 138 (1998).
[11] J. L. Cardy and U. C. Täuber, Phys. Rev. Lett. **77**, 4780 (1996).
[12] J. L. Cardy and U. C. Täuber, J. Stat. Phys. **90**, 1 (1998).
[13] P. Grassberger and K. Sundermeyer, Phys. Lett. **77B**, 220 (1978); J. L. Cardy and R. L. Sugar, J. Phys. A **13**, L423 (1980).
[14] H. J. Kreutzer, *Nonequilibrium Thermodynamics and Its Statistical Foundations* (Oxford Science Publication, Oxford, 1981).
[15] L. Frachebourg and P. L. Krapivsky, Phys. Rev. E **55**, 252 (1997).